

2016

## Formation of Double Ridges on Europa due to Viscoelastoplastic Deformation above Crystallizing Cryovolcanic Intrusions

Dougal Hansen  
*Portland State University*

**Let us know how access to this document benefits you.**

Follow this and additional works at: <https://pdxscholar.library.pdx.edu/honorstheses>

---

### Recommended Citation

Hansen, Dougal, "Formation of Double Ridges on Europa due to Viscoelastoplastic Deformation above Crystallizing Cryovolcanic Intrusions" (2016). *University Honors Theses*. Paper 318.

[10.15760/honors.267](https://pdxscholar.library.pdx.edu/honors/10.15760/honors.267)

This Thesis is brought to you for free and open access. It has been accepted for inclusion in University Honors Theses by an authorized administrator of PDXScholar. For more information, please contact [pdxscholar@pdx.edu](mailto:pdxscholar@pdx.edu).

Formation of Double Ridges on Europa  
Due to Viscoelastoplastic Deformation above Crystallizing Cryovolcanic Intrusions

By

Dougal Hansen

An undergraduate honors thesis submitted in partial fulfillment of the

requirements for the degree of

Bachelor of Science

in

University Honors

and

Geology

Thesis Adviser

Maxwell Rudolph

Portland State University

2016

## Abstract

Jupiter's moon Europa is comprised of an icy shell and a ~100 km thick global ocean overlying a rocky core. Among the myriad topographic features etched across its enigmatic surface, double ridges, which consist of two raised flanks with a central trough, are the most pervasive. Often running for hundreds of kilometers, they frequently overprint and offset pre-existing features and appear to be genetically related to cracks in the icy shell. Yet, after nearly two decades of study, these ridge systems and the processes through which they form remain incompletely understood. Several mechanisms have been proposed for ridge formation, one of which is that they are the surface expression of cryovolcanic dikes. Previous mechanical models have considered the elastic response of the icy shell above a crystallizing cryovolcanic intrusion. We present results from numerical models in which we treat the ice shell as a viscoelastoplastic medium and explore the variability of topographic expression due to varying rates of intrusion, tectonic extension, the initial width and depth of the dike. The irreversible viscous and plastic response of Europa's ice shell during intrusion allows large-amplitude topography to develop. However, we produce no topography comparable to double ridges on Europa.

## 1. Introduction

Among the features etched across Europa's surface, double ridges are the most pervasive, yet after nearly two decades of study, they remain incompletely understood. Double ridges, which consist of two raised ridges separated by a shallow, V-shaped trough, can stretch for hundreds of kilometers, intersect or truncate other ridge formations, or exist together in large groupings across vast plains. Double ridges belong to the class of surface features on Europa called lineae. These features, which include single ridges, complex ridges, cycloidal ridges, and ridge plains, often vary noticeably from double ridges when observed on a larger regional scale, but all share a strong morphological resemblance on a scale of a few kilometers (*Coulter, 2009*). These physical similarities possibly allude to similar processes driving their formation, and it is postulated that ridge features initiate as fractures within the ice shell and then evolve into the observed surface features under the influence of other mechanisms (*Prockter and Patterson, 2009*).

Several mechanisms have been proposed for ridge formation, one of which is that they are the surface expression of cryovolcanic dikes. Previous mechanical models have considered the elastic response of the icy shell above a crystallizing cryovolcanic intrusion (*Turtle, 1998; Dombard et al, 2013; Johnston and Montési, 2014*). Here, we present results from numerical models in which we treat the ice shell as a viscoelastoplastic medium and explore the variability of topographic expression due to varying rates of intrusion, dike geometry, and tectonic extension. In section 2, we provide evidence for the existence of a subsurface global ocean on Europa and the presence of liquid water within its icy shell, as these two features are foundational to our model. Section 3 summarizes the observed morphology of double ridges and outlines the basic principles and shortcomings of previous models that sought to explain their genesis. In section 4, we detail the

theory and methods used in our study. In sections 5, 6, and 7, we present our results, discuss the geological implications of our study, and state our conclusions.

## 2. Presence of liquid water on Europa

Even prior to the Voyager missions, researchers postulated that a global ocean of liquid water might underlie Europa's icy crust. This question of whether or not liquid water exists beneath the surface of this Jovian satellite is of great importance, since liquid water is held to be a prerequisite for life (*Reynolds et al., 1983; Chyba and Phillips, 2002*). Furthermore, the presence of a relatively warm convecting liquid underlying a cold, brittle shell would result in a unique set of geologic conditions that could possibly induce active tectonic processes analogous to those observed on Earth, such as spreading ridges, subduction zones, and even cryovolcanism (*Crawford and Stevenson, 1988; Kattenhorn and Prockter, 2014*). Mounting evidence gathered over the past two decades has added much credence to this hypothesis.

Evidence pointing to the existence of a global ocean is multi-faceted. Prior to the Voyager missions, *Consolmagno (1975)* hypothesized that tidal forces acting on Europa's rocky interior might provide enough energy to melt ice at the rock/ice boundary and sustain a body of liquid water. Later speculation revolved around surface features visible in photos returned from the Voyager and Galileo missions. Linear, crack-like ridge and band features (known collectively as *lineae*) are ubiquitous across the surface, and in many images, surface features were seen to be laterally offset across ridges, indicating strike-slip motion along fractures in the icy shell. Further support came from the discovery of chaos terrains in high resolution photos taken by the Galilean probes (~ 26 m/pixel). These highly broken-up regions on Europa's surface consist of jagged plates of preexisting terrain entrained in an irregular matrix, and when reconstructed, the plate fragments often fit together like pieces of a puzzle (*Alexander et al., 2009*). These features strongly allude to the presence of liquid water beneath the ice at the time of formation, and most models proposed to explain them take into account an underlying global ocean. However, the presence of a modern sub-ice ocean cannot be inferred from surface features alone since a hypothesized paleo-ocean could have frozen solid in the time elapsed since their genesis. Thus, the strongest argument for a current global ocean stems from the discovery a time-varying, induced magnetic field surrounding Europa, which was observed during the Galileo flybys (*Kivelson et al., 1997, 2000*). Predicted by *Kargel and Consolmagno (1996)*, this field strongly indicates a conducting, briny ocean near the moon's surface.

The existence of a sub-ice global ocean on Europa today is widely accepted; however, its exact nature, such as its composition and thickness relative to the overlying ice shell, remains elusive. Proposed models concerning ice shell thickness fall into two categories: A "thin-ice model," in which 2-5 km thick ice shell overlies a deep global ocean, or a "thick-ice model," in which a 10-30 km ice shell, comprised of a cold, thin brittle layer atop a warm ductile layer, overlies an ocean approximately 100 km deep. Constraining these parameters is imperative when considering the morphology of Europa's surface features since the conditions and stress fields required to produce them vary greatly for different shell thicknesses.

Assuming the presence of a subsurface ocean on Europa, the extent of liquid water can move through cracks in the ice is uncertain. The presence of water within the ice shell is supported by the surface morphology of Conamara chaos (*Schmidt et al., 2011; Sotin et al., 2002; Michaut and Manga, 2014*). Cracks in the shell originate through tensile stresses induced by tidal forces, nonsynchronous rotation, polar wander, or a pressurized ocean. However, the extent to which these fractures propagate remains uncertain since this process is highly dependent upon the thickness and composition of the shell (*Rudolph and Manga, 2009; Prockter and Patterson, 2009*).

*Manga and Wang (2007)* demonstrated that cracks could originate along the base of the shell due to stresses exerted against the ice by an underlying pressurized ocean. Europa's thermal gradient causes water to freeze from the outside in, and the volumetric expansion of ice effectively pressurizes the remaining liquid beneath. Being incompressible, the water exerts an equal and opposite force on the overlying ice, causing the shell to expand and fracture once the applied stress exceeds the strength of ice. Cracks at the ice-water interface would act as conduits for pressurized water to move upward until the water refroze or reached equilibrium. In the presence of ocean overpressure, the maximum extent of a water-filled fracture would slightly exceed neutral buoyancy, or  $\sim 90\%$  of the shell's thickness (*Manga and Wang, 2007*).

### **3. Morphology and proposed formation mechanisms**

#### *3.1. Morphology of ridge features.*

Given the shared morphological characteristics between double ridges and the other ridge features on Europa, classification schemes have been proposed to explain their relation. *Greenberg et al. (1998)* and *Head et al. (1999)* suggest that ridge features first originate as fractures in the icy crust, then form raised-flank troughs, then transition to double ridges, and finally evolve into more complex morphologies, such as complex ridges and ridge plains. This hypothesis is directly supported by observations of ridge systems that transition from crack to double ridges along strike. However, despite obvious similarities, the full relationship between each class of features remains shrouded in uncertainty.

As noted previously, double ridges are characterized by two raised, relatively symmetrical crests separated by a V-shaped, axial trough. These features can vary in length, width, and height by an order of magnitude, ranging from tens to hundreds kilometers long;  $\sim 200$  m to  $> 4$  km wide; and tens of meters to  $\sim 400$  m high (*Greeley et al., 2000*). The overall shape of double ridges often remains relatively constant over the duration of their length, and they can exist in nearly straight lines over long distances (*Prockter and Patterson, 2009*). Evidence of mass wasting can be found along ridge flanks, including boulders and dark talus deposits (*Moore et al., 2009*). Using photogrammetry techniques, *Coulter (2009)* observed the outside slopes of double ridges to be less than 28 degrees. If true, this would effectively rule out mass wasting as a principle mechanism of double ridge formation and require a subsurface mechanism to explain their morphology. However,

it is worth noting that photogrammetry can be uncertain when applied to Europa, since the technique relies on the composition and albedo of a surface in order to assess relative brightness and these parameters are not well constrained for double ridge flanks.

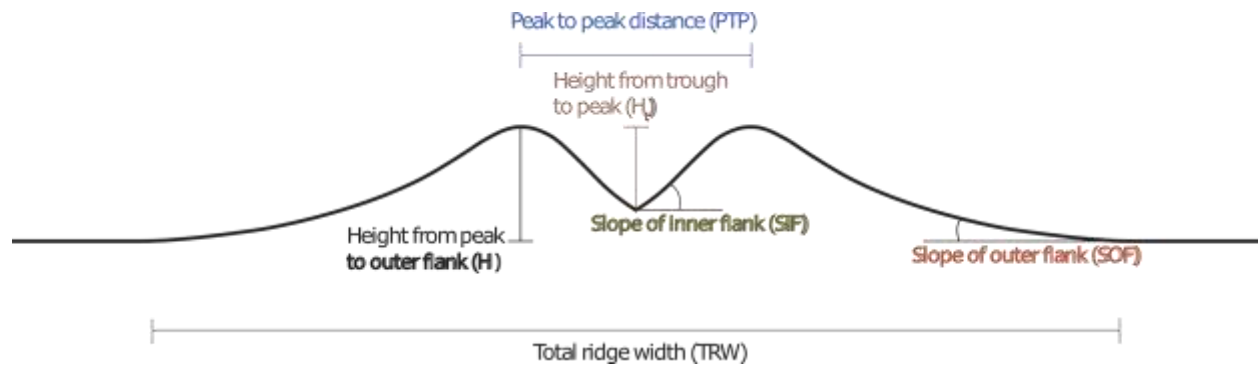


**Figure 1.** Anatomy of a double ridge

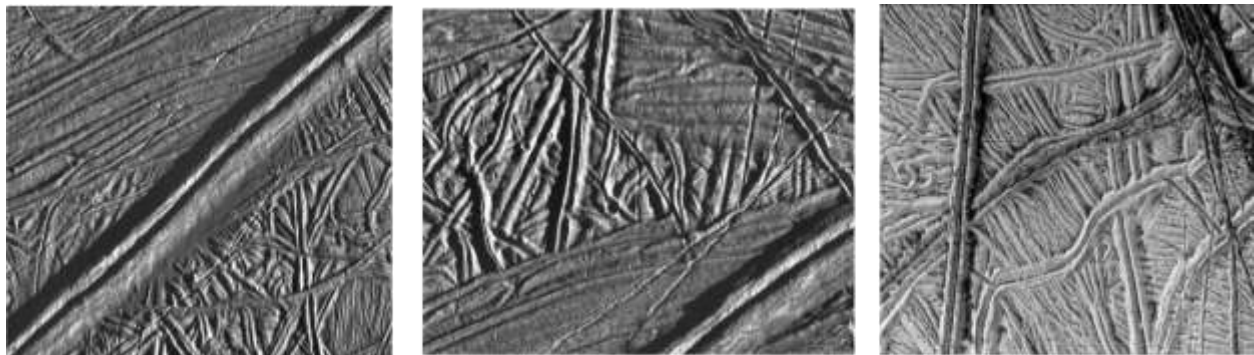


**Figure 2.** Variation within ridge systems on Europa. (Left image) Prominent, fully formed double ridge. (Center image) A series of fractures transect a plane of overlapping ridges with clear off-set seen along strike for certain ridges (Right image) Mature ridge plain comprised of a plethora of parallel and cross cutting ridges, often in running in pairs. Galileo images PIA00589, PIA01178, PIA00849.  
<http://photojournal.jpl.nasa.gov/catalog/>

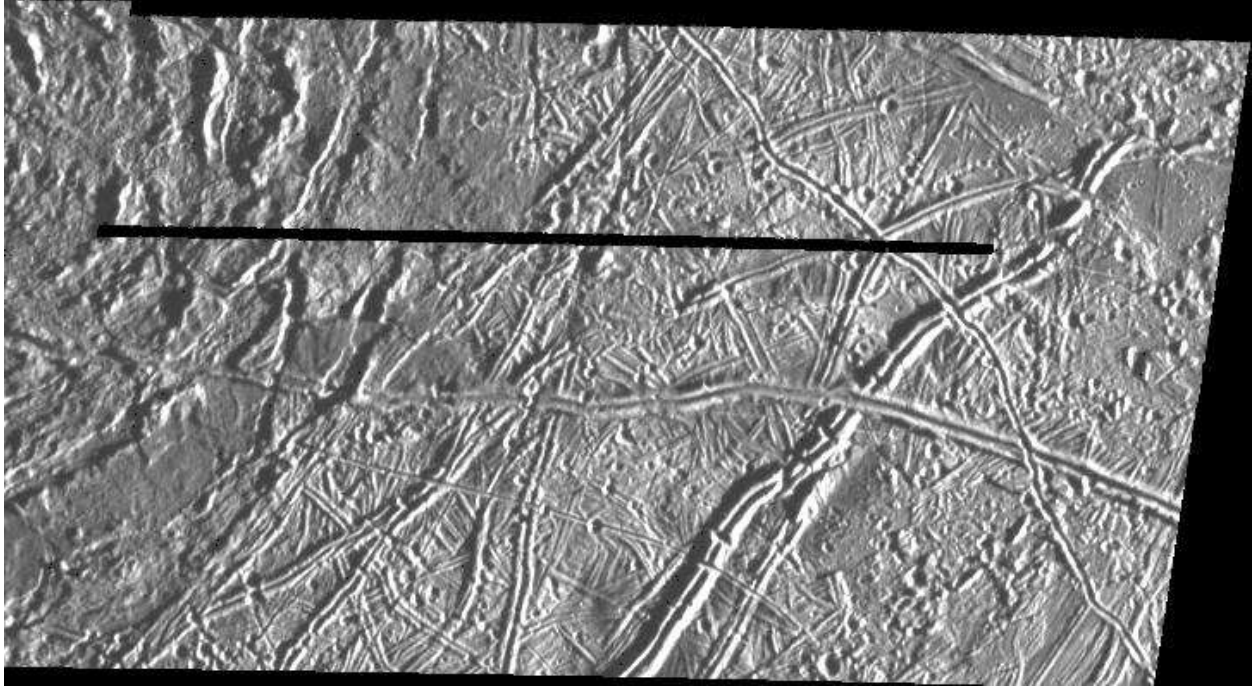


**Figure 3.** A ridge system transitioning along strike from a simple trough to proto-ridge to fully formed double ridge transects the center of this image. The image spans an area of 48 km x 91 km.  
<http://photojournal.jpl.nasa.gov/catalog/>

### *3.2. Formation mechanisms*

Several mechanisms have been presented to explain the formation of double ridges, ranging from accumulation of material through cryovolcanism, "tidal pumping", thermal buoyancy due to shear heating along fractures, and deformation above crystallizing water bodies within the shell. These models all succeed to an extent with explaining some facet of ridge morphologies, but all fall short to some degree when tested against observations (*Prockter and Patterson, 2009*). Indeed it is possible that perhaps multiple mechanisms work in tandem to create these features.

Proponents of cryovolcanism as a mechanism for ridge formation point to similarities between levees that form on the flanks of effusive lava flows on Earth and the double ridge systems on Europa (*Kadel et al., 1998*). The viability of this line of reasoning, however, is problematic because resemblance is purely superficial and even then only to an extent. In analogous lava flows on earth, flanking levees are not continuous over the duration of the flow and are often punctuated by other volcanic features such as spatter cones or secondary lava flows that emanate from the levee. Such features are contrary to what is observed on Europa as double ridges are often uniform along strike regardless of the surrounding topography. Furthermore, levee systems on Earth appear as two raised crests separated by a flat channel, whereas double ridges are separated by a distinct V-shaped trough (*Johnston and Montési, 2014*).

In the "tidal pumping" model initially proposed by *Pappalardo and Coon (1996)* and expounded upon by *Greenberg et al. (1998)* and *Tufts et al. (2000)*, cracks would propagate through Europa's shell as a result of diurnal tidal stresses from Jupiter and penetrate through to the ocean beneath. As tidal stresses cycled between extensional and compressive phases, water would be forced into the fractures at the bottom of the shell, partially freeze to a water-ice mixture, and then be expelled onto the surface as crack squeezes shut. Over many successive cycles, it is hypothesized that the accumulation of material on the surface along the flanks of the crack would resemble double ridges. In certain respects, this model is enticing: It correlates somewhat to processes that create pressure ridges in sea ice on Earth, and it can account for the linearity of ridges and many small-scale features found in conjunction with them (*Prockter and Patterson, 2009*). However, the calculated tidal stresses imposed on Europa from the Jovian system are neither sufficient to propagate a crack deep enough to reach the sub-ice ocean (*Crawford and Stevenson, 1988; Hoppa et al., 1999a; Lee et al., 2003*) or wide enough to expel the volume of water needed to create a double ridge assuming the fracture managed to reach a body of liquid water (*Lee et al., 2005*).

The shear heating model presents a stronger hypothesis than tidal pumping since it does not require cracks to penetrate the full thickness of Europa's icy shell and seems to account for the observed morphologies of double ridges. In this scenario, diurnal tidal stresses result in strike-slip motion along fractures in the shell, and the resultant frictional heating along the crack warms subsurface ice, causing uplift due to thermal buoyancy and possibly even melt along the fault (*Gaidos and Nimmo, 2000; Nimmo and Gaidos, 2002*). However, this model does not account for the eventual subsidence of the buoyantly uplifted ridges once the system has reached thermal equilibrium, and it becomes problematic in the context of complex ridge systems, since this mechanism would be expected to destroy previous ridges and observation points to their preservation (*Johnston and Montési, 2014*).

Multiple studies have explored the possibility that double ridges form through deformation above cryomagmatic intrusions (*Turtle et al., 1998a; Dombard et al. 2013; Johnston and Montési, 2014*), yet each of these studies falls short of providing a complete picture. *Turtle et al. (1998a)* suggest that a near-surface cryovolcanic intrusion, growing 1 m every tidal cycle would create ridges through ductile deformation of the surrounding ice shell. One major issue with this interpretation is that one expects the response of cold (110 K) near surface ice to a dike growing on a diurnal times would be brittle failure instead of plastic creep. *Dombard et al. (2013)* utilize a flexure model to test various ridge formation hypotheses that predict a thermal anomaly within the shell. After calculating heat flow and simulating flexure in the presence of these anomalies, they compare the resultant surface strain the placement of flanking fractures observed for certain double ridges on. Their simulations suggest that a cryovolcanic sill can produce a thermal anomaly and a locally thin shell that is consistent with flanking fractures observed in conjunction with certain double ridges. However, their model does not provide an explicit ridge formation mechanism as it relates to cryomagmatic sills; rather, it merely asserting that observed flexure at ridges deduced from flanking fractures may indicate sill emplacement. Furthermore, such flanking fractures exist only for a small percentage of ridge systems, casting doubt on sill emplacement



being an integral part of ridge formation (Coulter, 2009). Johnston and Montési (2014) treated the shell as an elastic medium and looked at the deformation caused by the volumetric expansion of a crystallizing water intrusion. They produced features with a similar morphology to double ridges on Europa; however, they did not account for the brittle failure of ice under stress regimes that exceed the yield strength of the shell.

## 4. Model and Methods

### 4.1. Theory

We employ a numerical, thermomechanical, viscoelastoplastic, two-dimensional code to solve equations governing fluid flow. This script is an adaption of a code by Gerya (2010), in which we change the boundary conditions and parameters to reflect the specific criteria of our model. Utilizing a finite-difference method in conjunction with a marker-in-cell technique, we solve the equations for the conservation of mass and momentum given by

$$\frac{\partial u_i}{\partial x_i} = 0$$

$$\frac{\partial \sigma'_{ij}}{\partial x_j} - \frac{\partial P}{\partial x_i} + \rho g_i = 0$$

where  $u_i$  is velocity,  $\sigma'_{ij}$  is the deviatoric stress tensor,  $P$  is pressure,  $\rho$  is density,  $g$  is gravity,  $x_i$  is a spatial coordinate, and  $i$  and  $j$  are the coordinate indices.

We implement a viscoelastoplastic rheology for Europa's ice shell. The behavior of ice is complex, involving several different Newtonian and non-Newtonian deformation mechanisms. However, a viscoelastoplastic rheology offers a reasonable first order approximation. Under this regime, ice will exhibit viscous, elastic, plastic, or brittle behavior depending on the timescale, confining pressure, temperature, and applied deviatoric stress involved.

For the viscoelastic component of this rheology, stress and strain are related through Maxwell's model. The total rate of strain can be decomposed into an elastic strain rate and a viscous strain rate, such that

$$\dot{\epsilon}'_{ij} = \dot{\epsilon}'_{ij(\text{elastic})} + \dot{\epsilon}'_{ij(\text{viscous})}$$

where,

$$\dot{\epsilon}'_{ij(\text{elastic})} = \frac{1}{E} \frac{D\sigma'_{ij}}{Dt}$$

$$\dot{\epsilon}'_{ij(viscous)} = \frac{1}{2\mu} \sigma'_{ij}$$

where  $E$  is Young's modulus, and  $\mu$  is viscosity. The style of deformation depends on a characteristic timescale for the material known as the Maxwell relaxation time, given by

$$T_m = \frac{\mu}{G}$$

where  $T_m$  is the Maxwell time,  $\mu$  is viscosity, and  $G$  is the elastic shear modulus. If deformation occurs on a relatively short timescale compared to  $T_m$ , a viscoelastic solid exhibits elastic behavior; conversely, irreversible viscous flow occurs on timescales much longer than the Maxwell time. Assuming a viscosity of  $10^{18}$  Pa-s and a shear modulus of  $1 \times 10^9$  Pa, this corresponds to a timescale  $T_m = 30$  years for surface ice on Europa.

The plastic component of the viscoelastoplastic rheology assumes an absolute shear stress  $\sigma_{yield}$  exists above which a material will undergo plastic yielding or brittle failure depending on the magnitude of the confining pressure. This critical stress  $\sigma_{yield}$  is given by

$$\sigma_{yield} = C + \sin(\phi)P$$

where  $C$  is the cohesion,  $P$  is Pressure, and  $\phi$  is the angle of internal friction. If the confining pressure is low and the strain rate is high, a viscoelastoplastic solid will behave elastically until the deviatoric stress exceeds the material's strength at which point the material will fracture. However, if the confining pressure and deviatoric stress approach  $\sigma_{yield}$ , the style of deformation will transition from recoverable elastic strain to irreversible plastic creep marked by highly deformed shear zones bounded by regions of low strain. As this stress-strain relationship depends only on the magnitude of the load applied and not on the rate of deformation, it is said to be time-independent.

Total strain rate for a viscoelastoplastic solid is comprised of three superimposed strain rates: a linear elastic strain rate produced by the rate of change of stress, a linear viscous strain rate, and a non-linear plastic strain rate, such that

$$\dot{\epsilon}'_{ij} = \dot{\epsilon}'_{ij(elastic)} + \dot{\epsilon}'_{ij(viscous)} + \dot{\epsilon}'_{ij(plastic)}$$

where,

$$\dot{\epsilon}'_{ij(plastic)} = 0 \text{ for } \sigma_{II} < \sigma_{yield}$$

$$\dot{\epsilon}'_{ij(plastic)} = \chi \frac{\sigma'_{ij}}{2\sigma_{II}} \text{ for } \sigma_{II} \geq \sigma_{yield}$$

$$\sigma_{II} = \sqrt{\frac{1}{2} \sigma'_{ij}{}^2}$$

where  $\sigma_{II}$  is the second deviatoric stress invariant,  $\sigma_{yield}$  is the plastic yield strength for a material, and  $\chi$  is the plastic multiplier, which satisfies the plastic yielding condition  $\sigma_{II} = \chi \sigma_{yield}$  (Gerya and Yuen, 2007).

#### 4.2. Model setup

Figure 4 illustrates the geometry of our model. All calculations were conducted in a two-dimensional Cartesian box with width ( $w$ ) by height ( $h$ ). Because Europa's ice shell is much thinner than its radius and we confine our domain to a shallow region at the shell's surface, a rectangular geometry is justified. The length to width aspect ratio is 5:1 with grid lines spaced evenly at resolutions of 191 x 61, or 381 x 121 depending on the initial width of the intrusion. We performed resolution tests to explore the effect of grid resolution on model behavior. From these tests, we determine that the resolution must be set such that initial geometry of intrusion is at least two cells wide.

We represent Europa's ice shell as a cold, brittle surface layer overlying a warmer, ductile layer. This presents a major uncertainty in our model as the thickness of the brittle surface layer is directly related to the total thickness and temperature gradient of the shell. However, for our purposes, we assign a thicknesses of 2 km and 4 km for the brittle layer, which corresponds to a 20 and 40 km thick shell based on our analysis of the Maxwell time for a conductive ice shell. Finally, we assign the upper portion of the domain as "sticky air," a low viscosity, low-density fluid commonly used to simulate free-surface conditions.

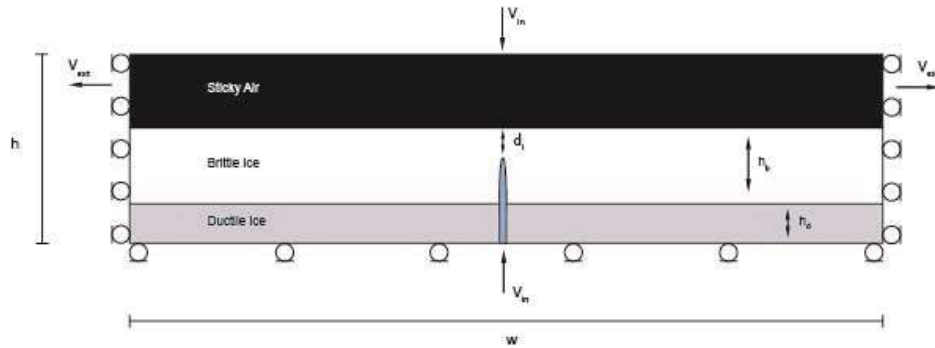


**Figure 4:** Model schematic as described in section 4.1. A cryovolcanic dike intrudes through a ductile ice layer of thickness  $h_d$  into a cold brittle ice layer of thickness  $h_b$ . The domain is 5 x 20 km and  $d_i$  represents the depth from the surface of the shell to the tip of the intrusion. Material flows into the dike at velocity  $v_{in}$ , and  $v_{ext}$  is the extensional strain rate.

Along the left/right bounds of the domain, we implement free-slip conditions in the vertical direction and prescribe velocity in the horizontal direction, and we apply the converse along the top/bottom borders. We define a viscoelastic timestep of one year, chosen to be longer than the Maxwell time of rheologically weakest material and significantly shorter than the Maxwell time of the strongest material. We carry out the simulation for 1500 years. In these calculations, we neglect the temperature dependence of viscosity, assigning instead a constant value for each material. Ice at Europa's surface has a viscosity of  $\sim 10^{20}$  Pa s (*Nimmo and Manga, 2009*). Numerical stability requires that the overall variation of viscosity is  $O(10^3)$  (*Gerya, 2009*). The viscosity contrast between rheologically weakest and strongest materials (i.e. the sticky air and the brittle layer) is  $10^4$  with contrast on the order of  $10^1$ - $10^2$  between each successively stronger material. Table 1 lists the mechanical properties adopted for these calculations.

We simulate inflow into a pre-existing water/ice dike and then observe the resultant topographic expression. We define a dike at the center of the domain, which intrudes vertically through the ductile layer into the base of the brittle layer, and inject material into it at a prescribed velocity. The inflow velocity, thickness of the brittle ice layer, geometry and depth of the dike, and the viscosity of the intruding material, are explored systematically to investigate their effect on topography.

**Table 1. Parameter values**

Name	Symbol	Value
Acceleration of gravity	$g$	$1.315 \text{ m s}^{-1}$
Density	$\rho$	$934 \text{ kg m}^{-3}$
Angle of internal friction	$\phi$	$36.9^\circ$
Thickness of brittle shell	$h_b$	$1.2\text{-}4 \text{ km}$
Shear modulus	$G$	$10^9 \text{ Pa}$
Viscosity of brittle layer	$\eta_b$	$10^{20} \text{ Pa S}$
Viscosity of ductile layer	$\eta_d$	$10^{19} \text{ Pa S}$
Viscosity of intrusion	$\eta_i$	$10^{17} \text{ or } 10^{18} \text{ Pa}$

## 7. Results

In adequately resolved simulations, no cases produce topography morphologically similar to double ridges on Europa. Instead, we categorize all features as single ridges, grabens bounded by normal faults, or uplifted fault blocks along reverse faults. Above a threshold inflow velocity around  $10^{-8}$  m/s, the rate of inflow dominates the evolution of the system, and the effects of other parameters were negligible for the range of values explored. We observe that at these velocities, material from the dike breaches the shell's surface, either as a single ridge or as the driver behind

rapidly uplifted, deformed ice blocks. Conversely, we observe that an inflow velocity an order of magnitude smaller failed to produce any topography other than a broad gradual uplift without brittle fracture.

For most inflow rates on the order of  $10^{-9}$  m/s, however, other parameters control the outcome, such as the initial width of the dike, the thickness of the ice lithosphere, and the depth of the intrusion below the shell's surface. We performed calculations using both a 4 km and a 2 km thick ice lithosphere. For cases with a 4 km thick brittle ice layer, inflow into a 400 m dike at velocities less  $10^{-8}$  m/s formed grabens through subsidence along opposing normal faults, whereas with 2 km thick ice lithosphere, intrusions wider than 120 m led to reverse faulting, uplift, and extrusion.

Although variation in the extent of faulting and resultant topography exists between graben-forming cases based on their specific initial conditions, these simulations all evolve similarly. Material injected into the base of the dike first accumulates as a wedge-shaped intrusion below the brittle ice layer, expanding the dike's width at the bottom of the domain from order  $10^2$  m to order  $10^3$  m. As the intrusion expands, induced stresses eventually exceed the strength of the ice, and conjugate normal faults extend rapidly from the base of the brittle layer to shell's surface. Further inflow of material results in both regional uplift above the dike and extensional strain, which is accommodated through lateral movement along these fault planes, eventually creating a shallow graben feature or even a series of staggered half grabens bounding a central down-dropped basin (Figure 6). Figure 5 illustrates the effect of depth of the intrusion on the final topography. A shallow intrusion 300 m deep, accommodated extension and subsidence along a single normal fault; whereas a dike 800 m deep produced fault bounded grabens through the mechanism described above.

Increasing the rate of inflow to a velocity of  $10^{-8}$  m/s or greater facilitates a more rapid ascent of material through the dike and accelerates the topographic evolution. Compressive stresses concentrated at the base of the brittle layer lead to the formation of reverse faults on either side of the intrusion. Subsequent inflow is accommodated along these planes as the bounded ice block is uplifted and deformed (Figure 7).

At low resolution, several simulations produced features similar to double ridges. With increased resolution, the behavior of these cases changed to the formation of a graben. However, it is worth noting how the behavior of these systems diverge at low and high resolutions, since they share a similar trajectory yet produce disparate topography. This divergence is rooted in the nature of faulting that occurs in the brittle layer during the early stages of dike growth. At higher resolutions, strain concentrates in two opposing zones of weakness that flank the dike and fracture into normal faults. Similar zones exist at low resolution as well, but they are dominated by an arcuate region of accumulated strain above the intrusion that fractures to form a listric fault. Further uplift of the shell beneath the fault tilts the blocks away from each other, pulling the hanging wall block away from the detachment plane and causing its collapse as a rollover anticline. (Figure 8).

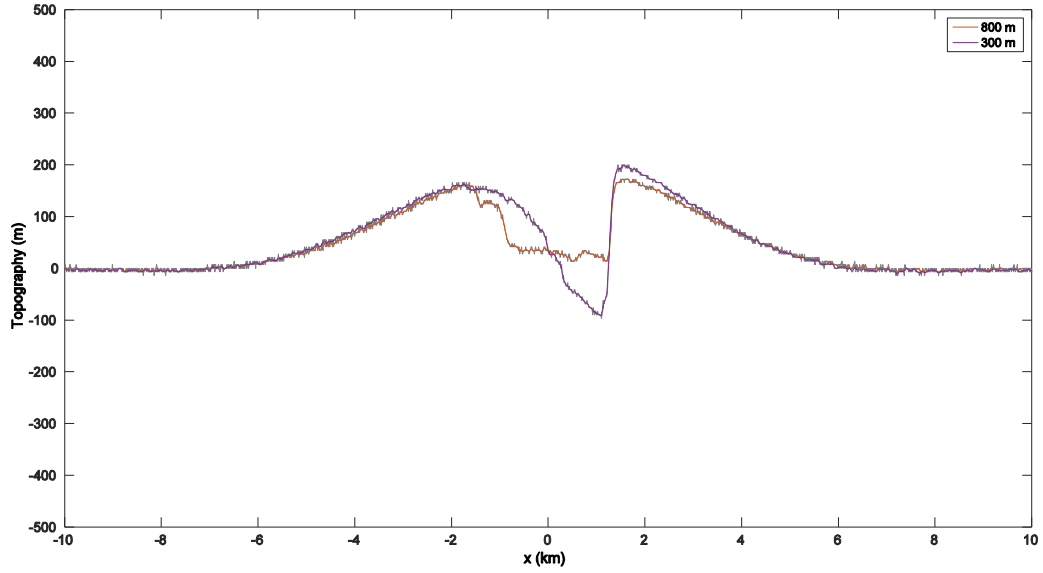
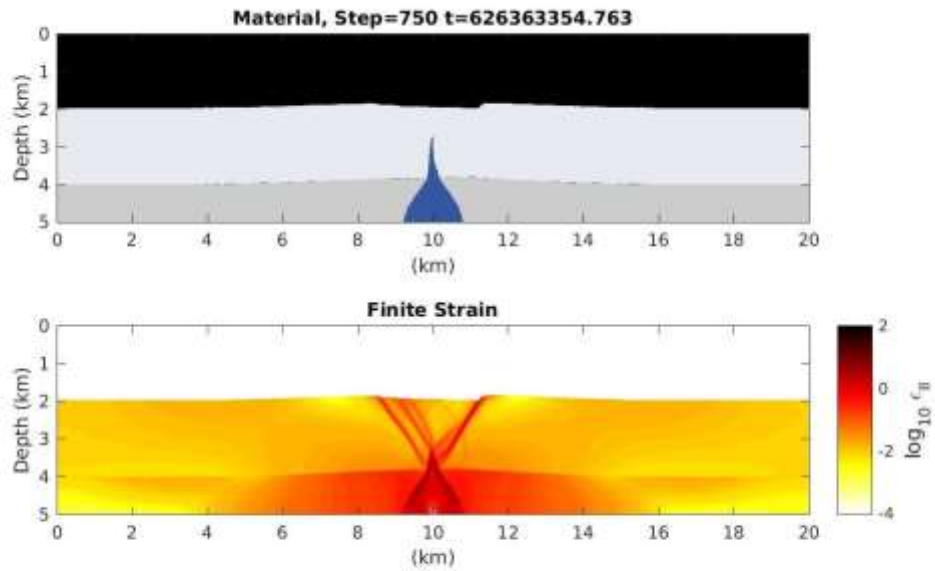


**Figure 5.** Effect of depth on topography. For both cases: initial dike width = 100 m; inflow velocity =  $5 \cdot 10^{-9}$  m/s; At 300 m deep, extension and uplift is accommodated along a single normal fault. At 800 m deep (Figure 6), a series of normal faults bound a central graben.

1.



2.

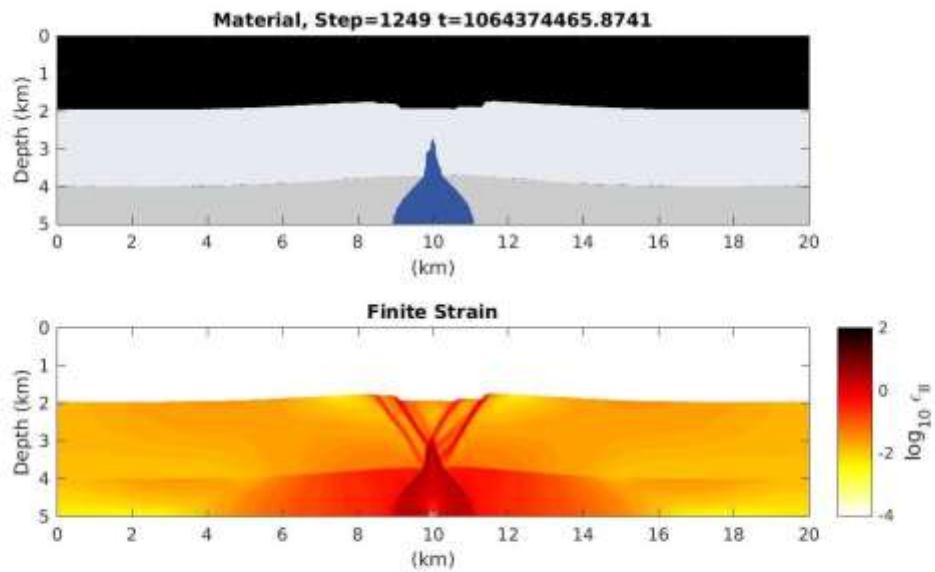
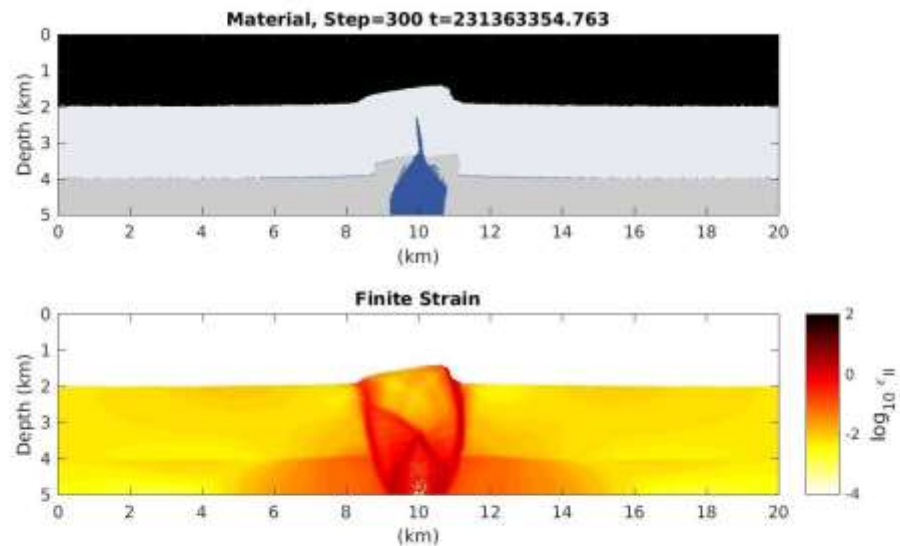


**Figure 6.** Evolution of a graben-forming simulation, shown at (1)  $t = 750$  yr and (2)  $t = 1249$  yr. Initial dike width = 100 m; inflow velocity =  $5 \cdot 10^{-9}$  m/s; depth of intrusion below surface = 800 m (1) As new material accumulates in a wedge below the base of the brittle ice layer, strain localizes in two opposing zones of weakness, leading to fracture and normal faulting. (2) Further inflow results in further faulting and regional uplift, producing a pair of fault bounded half-grabens flanking a central basin.

1.



2.

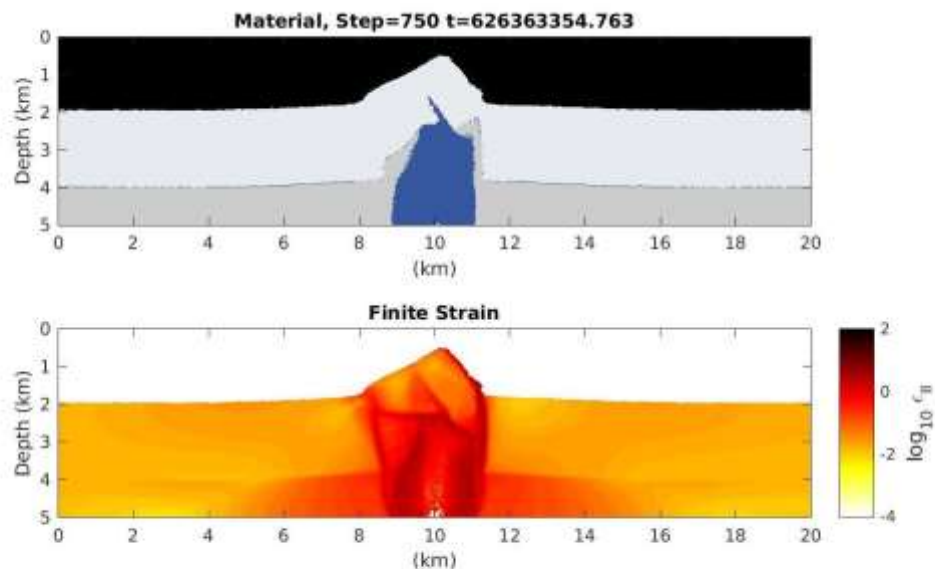
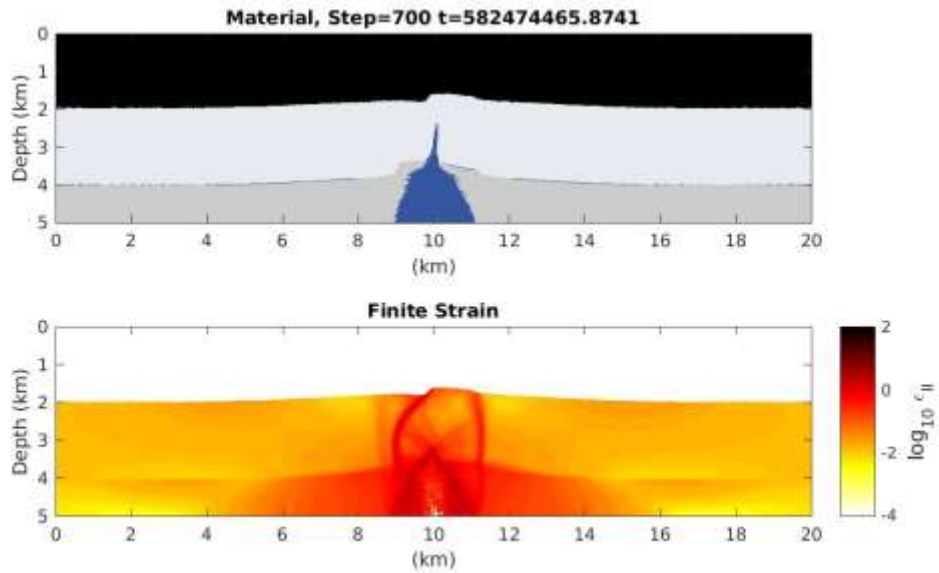


**Figure 7.** Evolution of a simulation producing uplift of ice blocks along reverse faults shown at (1)  $t = 300$  yr, (2)  $t = 750$ . Initial dike width = 200 m; inflow velocity =  $5 \cdot 10^{-8} \text{ m/s}$ ; (1) Compressive stresses concentrated against the base of the brittle layer lead to the propagation of reverse faults on either side of the intrusion. (2) Subsequent inflow is largely accommodated along these planes as the bounded ice block is uplifted and deformed.



1.



2.

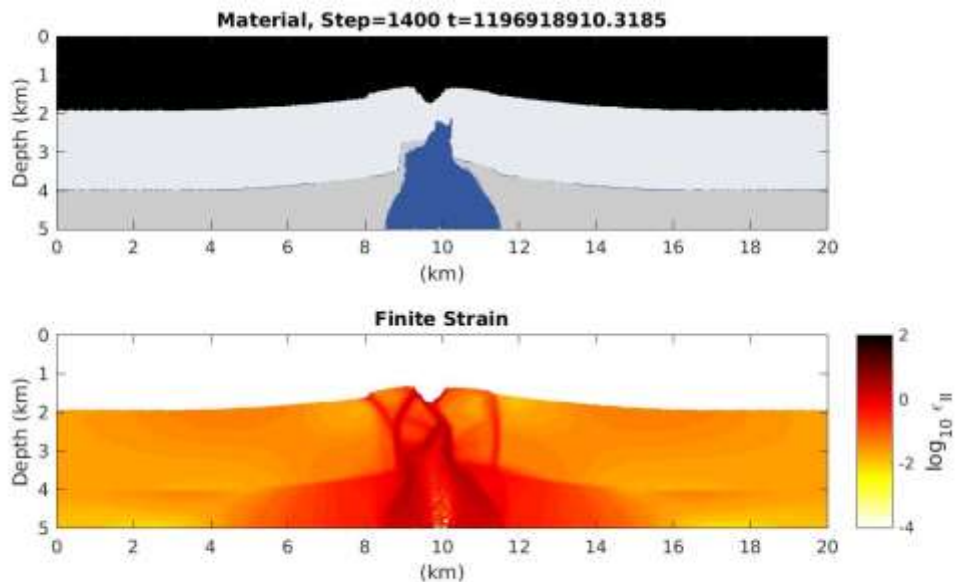


**Figure 8.** Evolution of a simulation that produces a double ridge at low resolution (1)  $t = 700$  yr and (2)  $t = 1400$  yr. Inflow velocity =  $5 \cdot 10^{-9}$  m/s ; Initial width of dike = 50 m ; Depth of intrusion = 800 m. (1) A listric fault propagates from the base of the brittle layer to the surface as the shell is wedged apart by the intrusion. (2) Further inflow results in both regional uplift above the dike and continued extension throughout the shell. These movements are accommodated along the fault plane, which forces the blocks to tilt away from each other. The fracture and subsequent uplift of a small block in the hanging wall increases the symmetry of the ridges.

## 6. Discussion

Single ridges and grabens are the most common topographic features produced through our calculations. However, given the physical constraints governing the movement of water through the ice shell, the emplacement of material on the shell's surface as a single ridge is unrealistic. Therefore, we neglect these cases from consideration. However, grabens, comprised of a down-dropped block flanked by opposing sets of normal faults, frequently form above intrusive dikes on Earth, Mars, and Venus, and numerous theoretical and physical models elucidate the mechanical effects of near-surface dike emplacement (*Pollard et al., 1983; Mastin and Pollard, 1988; Rubin and Pollard, 1988; Rubin, 1992; Coulter, 2009*). *Pollard et al. (1983)* showed that internal pressure generated by the accumulation of material within a dike compresses the surrounding material and produces horizontal elastic displacements emanating away from the intrusion. Due to the geometry and position of the dike, displacement is effectively zero directly above the intrusion and greatest at some distance away from either side of the dike's plane. This stress gradient results in two zones of maximum tension which flank the intrusion at the surface. If the resultant extensional stresses exceed the tensile strength of the material, two parallel zones of opposing normal faults will form on either side of the dike, facilitating further extension through down-drop of a center block along the fault planes (*Chadwick and Embley, 1998*).

*Turtle et al. (1998a)* proposed that the accumulation of material within a narrow vertical dike in Europa's ice shell could produce ridge-like surface features instead of grabens under specific boundary conditions. Based on their calculations using a viscoelastoplastic rheology, a dike growing 1 m in width every 80-hour tidal cycle would cause plastic failure in the ice and produce localized upward ductile deformation on either side of the crack that morphologically resembles double ridges. *Johnston and Montési (2014)* also produced ridge-like features by treating the ice shell as an elastic medium and modeling the deformation caused by the volumetric expansion of a vertically oriented, elliptical, crystallizing water body. However, the assumed behavior of the ice shell in both studies is problematic. Due to the low confining pressure and extreme cold temperatures on Europa, strain in near surface ice should be accommodated through brittle failure and subsequent movement along fault planes at stresses surpassing the shell's tensile strength. As both sets of calculations induced stresses exceeding this value, plastic creep or purely elastic deformation past that point is unrealistic. We observe a brittle response in our simulations, and evidence of brittle failure is ubiquitous across Europa's surface (*Coulter, 2009*).

Ring grabens, which encircle impact craters, are commonly observed across Europa's surface, and previous work has even utilized them as proxies to constrain the thickness of Europa's icy lithosphere (*Singer et al. 2013*). However, prominent linear graben features that persist in conjunction with double ridge systems or as separate entities are not directly observed. Certain dilation bands, referred to as fault bands, exhibit an interior fabric of fine linear striations. Previous work interpreted these features to be a sequence of grabens bounded by normal faults, which were subsequently inundated by extruded sub-surface material. According to this hypothesis, each

graben corresponds to a unique episode of regional extension (*Sullivan et al. 1998, Prockter et al. 1999, 2002, Stempel et al. 2005*). Although it is beyond the scope of our study to draw a comparison, it is interesting to note that several of our simulations evolved in a similar manner. Certain conditions, such as an imposed extensional strain with an initial dike width greater than 200 m, ultimately caused material from the dike to breach the shell's surface and inundate a newly formed graben.

Our model invokes the existence of a low-viscosity fluid-filled dike with a width on the order of  $10^2$  -  $10^3$  m near the surface of the shell, and we assume this system to be fed by a conduit connecting the dike to the ocean. However, problems arise when considering the mechanical implications of this scenario. Ridge systems that transition along strike from a surface fracture to a double ridge provide strong evidence that tensile cracks in Europa's shell represent the first stage in ridge development (*Coulter, 2009*). Therefore, when considering the role cryovolcanic dikes play in ridge formation, it is important to explain it in the context of these transitional ridge systems and the morphological relationship between surface cracks and double ridges.

Tensile fractures in Europa's shell primarily develop as a result superimposed extensional stresses induced through tidal pull and nonsynchronous rotation. Given the magnitudes of stress produced through these mechanisms, fractures cannot penetrate from the surface to the underlying ocean for an ice shell greater than 2.5 km thick (*Rudolph and Manga, 2009*). Consequently, any conduit from the ocean to the surface must propagate upwards from shell's base. Intruding water may utilize pre-existing cracks as regions of low resistance or propagate a crack through the shell through its phase change to ice (*Johnston and Montési, 2014*). Due to negative buoyancy of water, a cryovolcanic dike in Europa's shell could extend upward to a depth of  $\sim 90\%$  of the shell's thickness (*Manga and Wang, 2007*), although certain conditions, such as the presence of dissolved volatile gases, could potentially drive a water/ice mixture of a higher density than the shell closer to the surface (*Greenberg et al., 1998*). Yet even with the added stresses caused through overpressure and the injection of pressurized fluid at the crack tip, these constraints on crack propagation dictate that surface fractures, such as those in a transitional ridge system, must only extend downward through 1/10 of the ice shell thickness and therefore are unlikely to be connected to a subsurface ocean.

The successive intrusion and accumulation of material within a persistent cryovolcanic dike could produce surface fractures as well. Our results agree with previous models investigating the surface expression of dike emplacement in that the stress gradient at the shell's surface produced parallel sets of fractures flanking the dike instead of a single fracture directly above the intrusion (*Pollard et al., 1983; Mastin and Pollard, 1988; Rubin and Pollard, 1988; Rubin, 1992; Coulter, 2009*). Similar behavior can also be inferred from *Johnston and Montési's (2014)* results despite the limitations inherent in the purely elastic rheology they employed. In their cases that produced double ridges, the volumetric expansion of the dike also produced a stress field at the surface where two zones of maximum stress flank a zone of minimum stress directly overlying the intrusion. Given that these max stresses surpass the tensile strength of ice, one predicts fractures to form in a similar fashion to our simulations given a more realistic rheology.

The fractures produced in our simulations, however, differ markedly from the morphology of transitional ridges system observed on Europa. Traversing one of these features along strike from the simple fracture to the fully formed double ridge, one observes a single crack that ultimately aligns with the central trough of the double ridge of two parallel fractures that evolve into normal faults (*Coulter, 2009*). As such, it is difficult to appeal to a near-surface cryovolcanic dike as the mechanism driving the formation of these transitional ridge systems, assuming the simple fractures represent the first stage in ridge development.

Another problem arises when considering the evolution of the dike in our model. As discussed in Section 5.1, material preferentially accumulates near the bottom of the domain as a wedge shape, ultimately increasing the width of the intrusion from the order of  $10^2$  m to  $10^3$  m. This behavior is likely unrealistic for conditions on Europa. Conduits are expected to be far thinner (on the order of  $10^1$  m) and variable, opening and closing in response to cyclical extensional and compressional tidal stress (*Greenberg et al. 1998*). A more reasonable approach is taken by *Melosh and Turtle (2004)*, in which models cracks opening in response to tidal stresses facilitate the upward movement of water, which subsequently freezes along the walls of the fracture. Thus the accumulation of ice within the intrusion occurs incrementally in conjunction with Europa's diurnal tidal cycle rather than as a continuous flow of material into a rapidly expanding cryovolcanic dike.

## 7. Conclusions

In summary, we find the cryovolcanic dike hypothesis to explain double ridge formation on Europa to be problematic. Previous work attributes these features to localized ductile flow or elastic deformation above an intrusion. However, our models show that for the geometries, inflow velocities, and boundary conditions we implemented, intrusions do not evolve to form double ridges. Stresses induced by expanding near-surface water/ice dike cause brittle failure of the ice lithosphere and subsequent movement along fault planes. The nature of this faulting depends primarily on the rate of inflow and the initial width of the dike. Topography produced through our simulation (i.e. extruded cryovolcanic single ridges and normal fault bounded grabens) lacks clear analog on Europa. However, graben produced through our simulations conform to established dynamics of near-surface dikes on Earth, Venus, and Mars.

## References

- Alexander, C., Carlson R., Consolmagno G., Greeley R., and Morrison D., (2009) The exploration history of Europa. *Europa*. The University of Arizona Press, 3-26.
- Chadwick, W. W., Jr. and Embley, R. W. (1998), Graben formation associated with recent dike intrusions and volcanic eruptions on the mid-ocean ridge. *Journal of Geophysical Research*, *103*, 9807-9825
- Chyba, C.F. and Phillips, C.B. (2002) Europa as an abode of life. *Orig. Life Evol. Biosp.*, *32*, 47-68. <http://dx.doi.org/10.1023/A:1013958519734>
- Consolmagno, G. J. (1975) *Thermal History Models of Icy Satellites*. M.S. thesis, Massachusetts Institute of Technology, Cambridge. 202 pp.
- Coulter, C.E. (2009) *Kinematic and Morphological Evolution of Europa's Ridges*. M.S. Thesis, University of Idaho. 558pp.
- Coulter, C.E., Kattenhorn S.A., and Schenk, P.M. (2009). Topographic profile analysis and morphologic characterization of Europa's double ridges. *Lunar Planet. Sci. XL*. Abstract #1960.
- Crawford G. D. and Stevenson D. J. (1988) Gas-driven water volcanism and the resurfacing of Europa. *Icarus*, *73*, 66-79.
- Dombard, A.J., G.W. Patterson, A.P. Lederer, and L.M. Prockter, Flanking Fractures and the Formation of Double Ridges on Europa, *Icarus*, *223*, 74-81, 2013.
- Gaidos E. J. and Nimmo F. (2000) Tectonics and water on Europa. *Nature*, *405*. 637.
- Gerya T.V and Yuen D. A. (2007) Robust characteristics method for modeling multiphase visco-elasto-plastic thermos-mechanical problems. *Physics of the Earth and Planetary Interiors*, *163*, 83-105
- Greely R., Figueredo P.H., Williams D. A., Chuang F. C., Klemaszewski J. E., Kadel S. D., Prockter L. M., Pappalardo R. T., Head J. W. III, Collins G. C., Spaun N. A., Sullivan R. J., Moore J. M., Senske D. A., Tufts B. R., Johnston T. V., Belton M. J. S., and Tanaka K. L. (2000) Geologic mapping of Europa. *J. Geophys. Res.*, *105*, 22559-22578.

- Greenberg, R., Geissler P.E., Hoppa G., Tufts B. R., Durda D. D., Pappalardo R., Head J. W., Greely R., Sullivan R., and Carr M. H. (1998). Tectonic processes on Europa: Tidal stresses, mechanical response, and visible features. *Icarus*, 135, 64-78.
- Greenberg, R., Geissler P., Hoppa G., and Tufts B. R. (2002) Tidal-tectonic processes and their implications for the character of Europa's icy crust. *Rev. Geophys.*, 40, 1.1 to 1.33.
- Head J. W., Pappalardo R. T., and Sullivan R. (1999) Europa: Morphological characteristics of ridges and triple bands from Galileo data (E4 and E6) and assessment of a linear diapirism model. *J. Geophys. Res.*, 104. 24223-24236.
- Hoppa G. V., Tufts B. R., Greenberg R., and Geissler P. E. (1999a) Formation of cycloidal features on Europa. *Science*, 285, 1899-1902.
- Kadel, S., Fagents, S., Greeley, R., and Galileo SSI Team (1998) Trough-bounding ridge pairs on Europa – Considerations for an endogenic model of formation. *Lunar Planet. Sci. XXIX*. Abstract #1078.
- Kargel J. S. and Consolmagno G. J. (1996) Magnetic fields and the detectability of brine oceans in Jupiter's icy satellites. *In Lunar and Planetary Science XXVII*, pp. 643-644. Lunar and Planetary institute, Houston.
- Kattenhorn S. A. and Prockter L. M. (2014) Evidence for subduction in the ice shell of Europa. *Nature Geoscience*, 7. 762-767
- Kivelson M. G. Khurana K. K., Joy S., Russell C.T., Southwood D. J., Walker R. J., and Polanskey C. (1997) Europa's magnetic field signature: Report from Galileo's pass on 19 December 1996. *Science*, 276, 1239-1241.
- Kivelson M. G., Khurana K. K., Russell C. T., Volwerk M., Walker R. J., and Zimmer C. (2000) Galileo magnetometer measurements: A stronger case for a subsurface ocean on Europa. *Science*, 289. 1340-1343.
- Johnston S. A., and L. G. J. Montési (2014) Formation of ridges on Europa above crystallizing water bodies inside the ice shell. *Icarus*, 237, 190-201.
- Lee S., Zandolin M., Thode A. M., Pappalardo R. T., and Makris N. C. (2003) Probing Europa's interior with natural sound sources. *Icarus*, 165, 144-167.
- Lee S., Pappalardo R. T., and Makris N. C. (2005) Mechanics of tidally driven fractures in Europa's icy shell. *Icarus*, 177, 376-379.

- Manga, M. and Wang, C.-Y. (2007). Pressurized oceans and the eruption of liquid water on Europa and Enceladus. *Geophys. Res. Lett.*, *34*, L07202. <http://dx.doi.org/10.1029/2007GL029297>.
- Moore, J. M., Black G., Buratti B., Phillips C. B., Spencer J., and Sullivan R. (2009) Surface properties, regolith, and landscape degradation. *Europa*. The University of Arizona Press, 329-349.
- Nimmo F. and Gaidos E (2002) Strike-slip motion and double ridge formation on Europa. *J Geophys. Res.*, *107*, DOI: 10.1029/2000JE001476.
- Pappalardo R. T. and Coon M. D. (1996) A sea ice analog for the surface of Europa. In *Lunar and Planetary Science XXVIII*, pp. 997-998. Lunar and Planetary Institute, Houston.
- Pollard, D.D., Delaney, P.T., Duffield, W.A., Endo, E.T., and Okamura, A.T., 1983, Surface deformation in volcanic rift zones. *Tectonophysics*, *v. 94*, 541-584.
- Prockter, L. M. and Patterson G. W. (2009) Morphology and evolution of Europa's ridges and bands. *Europa*. The University of Arizona Press, 237-258.
- Reynolds R. T., Squyres S., Colburn D., and McKay C. (1983) On the habitability of Europa, *Icarus*, *56*, 246-254.
- Rubin, A. M. (1992), Dike-induced faulting and graben subsidence in volcanic rift zones. *J. Geophys. Res.*, *97(B2)*, 1839-1858
- Rubin, A.M., and Pollard, D.D., 1988, Dike-induced faulting in rift zones of Iceland and Afar. *Geology*, *v. 16*, 413-417.
- Rudolph M.L. and M. Manga (2009), Fracture penetration in planetary ice shells, *Icarus* *199(2)*, 536-541
- Sullivan, R., Greeley, R., Klemaszewski, J., Moreau, J., Tufts, B. R., Head, J. W., Pappalardo, R., Moore, J., 1999b. High resolution geological mapping of ridged plains on Europa. In *Lunar and Planetary Science Conference XXX*, Abstract #1925. Lunar and Planetary Institute, Houston (CD-ROM).
- Turtle, E. P., Melosh, H. J., Phillips, C. B., 1998a. European ridges: tectonic response to dike intrusion. AGU Spring Meeting, Abstract P51A-10.
- Tufts B. R., Greenberg R., Hoppa G., and Geissler P. (2000) Lithospheric dilation on Europa. *Icarus*, *146*, 75-97.

